

Software Development for Beam Cooling Simulation Including General Collider Physics

Interim report

I.N.Meshkov, A.O. Sidorin, A.V.Smirnov, G.V.Trubnikov
Joint Institute for Nuclear Research, Dubna, Russia

Abstract

General attention at this stage of the work was devoted to development of the electron cooling models in order to provide realistic comparison between nonmagnetized cooling force calculation and experiments at Fermilab Recycler ring. Algorithm for optical stochastic cooling simulation was introduced. The program structure was developed to realize detailed IBS simulation in accordance with Zenkevich and plasma models.

During this stage of the Accord realization the following new algorithms were introduced into BETACOOOL:

- numerical calculation of the cooling force in nonmagnetized electron beam in accordance with Binney's formulae,
- asymptotic formulae for friction force derived by Ya. Derbenev,
- simulation of envelope scalloping effect,
- direct simulation in BETACOOOL the voltage step method for friction force measurements,
- algorithm for longitudinal optical stochastic cooling simulation.

This report includes description of new models inserted into the code, results of benchmarking and brief description of stochastic cooling simulation developed in co-operation with FZJ and optical stochastic cooling simulation developed on the basis of BNL model.

Introduction

Initial design of RHIC electron cooling system presumed generation of magnetized electron beam and its injection after acceleration into solenoid providing longitudinal magnetic field of the value of 2 – 5 T. Large emittance of the electron beam prevents ion-electron recombination in the cooling section and electron magnetization provides large enough cooling force.

A few models for magnetized cooling simulation were developed in the frame of previous contract between BNL and JINR. The results of the magnetized friction force calculation were compared with simulation of ion dynamics in an electron cloud using VORPAL code and with especial experiments at CELSIUS cooling system. As result the accuracy of the cooling rate calculation was increased and disagreement between numerical models and experimental results does not exceed 50%. Simulations shown that for sufficient increase of the luminosity a required charge of the electron bunch should be about 20 nC.

Electron cooling at RHIC using non-magnetized electron beam sufficiently simplifies the cooler design. Generation and acceleration of the electron bunch without longitudinal magnetic field permits to reach low value of emittance in the cooling section. Suppression of the ion recombination with electrons in the cooling section can be performed using undulator at relatively small field ~ 10 -50 G. The cooling rate required for intrabeam scattering suppression can be obtained at small charge of the electron bunch ~ 2 -5 nC.

Obvious advantages of nonmagnetized version of the cooler design stimulate development and benchmarking of the algorithm for cooling force calculation in absence of the magnetic field. In previous version of BETACOOOL program for friction force calculation in nonmagnetized electron beam the following algorithms were used:

- numerical evaluation of 3D integral over the electron distribution function in the case of flattened velocity distribution,
- Chandrasekhar's formula for the friction force at uniform Maxwellian velocity distribution,
- asymptotic formulae for the friction force at flattened velocity distribution derived by Meshkov.

To provide accurate benchmarking of the existing algorithms and to improve accuracy and speed of the calculation two new algorithms were introduced into the code: Binney's formula and asymptotic representation by Derbenev for flattened velocity distribution.

The nonmagnetized electron beam is used for cooling of 8 GeV antiprotons at Recycler cooling system (Fermilab) commissioned in 2005. To provide comparison between friction force simulated with BETACOOOL and measured at Recycler the algorithm for direct simulation of the ion beam parameter evolution during a voltage step procedure was introduced into the code.

To provide more accurate simulations of Intrabeam scattering process the algorithm structure was modified. In the tracking procedure the longitudinal motion representation was corrected and tested. The modules for particle co-ordinate transformation from laboratory frame to beam frame and back were introduced. To avoid sufficient increase of the simulation time the possibility to change an integration step over time for each process independently was introduced.

To control the bunch length one planes to use an optical stochastic cooling system. Algorithm for the optical stochastic cooling simulation developed by BNL was implemented into the code. For simulation of usual stochastic cooling the model developed by FZJ can be used in the simulations. Description of this algorithm is also included into this report.

1. Friction force in nonmagnetized electron beam

1.1. Numerical calculation of the force components

In the particle rest frame the friction force acting on the ion at charge number Z inside a nonmagnetized electron beam at density of n_e can be evaluated by numerical integration of the following formula

$$\vec{F} = -\frac{4\pi n_e e^4 Z^2}{m} \int \ln\left(\frac{\rho_{\max}}{\rho_{\min}}\right) \frac{\vec{V} - \vec{v}_e}{|\vec{V} - \vec{v}_e|^3} f(v_e) d^3 v_e, \quad (1.1)$$

where e and m are the electron charge and mass, V and v_e are the ion and electron velocities respectively.

The Coulomb logarithm $\ln\frac{\rho_{\max}}{\rho_{\min}}$ is kept under the integral because the minimal impact parameter depends on electron velocity:

$$\rho_{\min} = \frac{Ze^2}{m} \frac{1}{|\vec{V} - \vec{v}_e|^2}. \quad (1.2)$$

At given value of the ion velocity the maximum impact parameter is constant and it is determined by dynamic shielding radius or the ion time of flight through the electron cloud. Radius of the dynamic shielding sphere coincides with Debye radius:

$$\rho_D = \frac{\Delta_e}{\omega_p}, \quad (1.3)$$

when the ion velocity is less than the electron velocity spread Δ_e . The plasma frequency ω_p is equal to

$$\omega_p = \sqrt{\frac{4\pi n_e e^2}{m}}. \quad (1.4)$$

When the ion velocity sufficiently larger than the electron velocity spread it determines the shielding radius

$$\rho_{sh} = \frac{V}{\omega_p}. \quad (1.5)$$

The both formulae (1.3) and (1.5) can be combined together to have a smooth dependence of the shielding radius on the ion velocity:

$$\rho_{sh} = \frac{\sqrt{V^2 + \Delta_e^2}}{\omega_p}. \quad (1.6)$$

In the case, when the shielding sphere does not contain big enough number of electrons to compensate the ion charge (such a situation takes a place in the case of magnetized electron beam at low longitudinal velocity spread) it has to be increased in accordance with the electron beam density and the ion charge. In the program this radius is estimated from the expression

$$n_e \rho^3 \sim 3Z. \quad (1.7)$$

As a result, the maximum impact parameter is calculated as a minimum from three values:

$$\rho_{\max} = \min \left\{ \max \left(\rho_{sh}, \sqrt[3]{\frac{3Z}{n_e}} \right), V\tau \right\}. \quad (1.8)$$

The second term describes the distance, which the ion passes inside the electron beam. Here τ is the ion time of flight the cooling section in the PRF:

$$\tau = \frac{l_{cool}}{\beta\gamma c}. \quad (1.9)$$

In the case of axial symmetry the electron distribution function can be written in the following form:

$$f(v_e) = \left(\frac{1}{2\pi} \right)^{3/2} \frac{1}{\Delta_{\perp}^2 \Delta_{\parallel}} \exp \left(-\frac{v_{\perp}^2}{2\Delta_{\perp}^2} - \frac{v_{\parallel}^2}{2\Delta_{\parallel}^2} \right), \quad (1.10)$$

where Δ_{\perp} and Δ_{\parallel} are the electron velocity spreads in the transverse and longitudinal direction correspondingly. The shielding cloud in this case has an ellipsoidal shape which can be approximated by the sphere of radius calculated using effective electron velocity spread:

$$\Delta_e^2 = \Delta_{\perp}^2 + \Delta_{\parallel}^2. \quad (1.11)$$

The components of the friction force (1.1) can be calculated in cylindrical co-ordinate system as follows:

$$F_{\perp} = -\sqrt{\frac{2}{\pi}} \frac{Z^2 e^4 n_e}{m \Delta_{\perp}^2 \Delta_{\parallel}} \int_0^{\infty} \int_{-\infty}^{\infty} \int_0^{2\pi} \ln \left(\frac{\rho_{\max}}{\rho_{\min}} \right) \frac{(V_{\perp} - v_{\perp} \cos \varphi) \exp \left(-\frac{v_{\perp}^2}{2\Delta_{\perp}^2} - \frac{v_{\parallel}^2}{2\Delta_{\parallel}^2} \right)}{\left((V_{\parallel} - v_{\parallel})^2 + (V_{\perp} - v_{\perp} \cos \varphi)^2 + v_{\perp}^2 \sin^2 \varphi \right)^{3/2}} v_{\perp} d\varphi dv_{\parallel} dv_{\perp},$$

$$F_{\parallel} = -\sqrt{\frac{2}{\pi}} \frac{Z^2 e^4 n_e}{m \Delta_{\perp}^2 \Delta_{\parallel}} \int_0^{\infty} \int_{-\infty}^{\infty} \int_0^{2\pi} \ln \left(\frac{\rho_{\max}}{\rho_{\min}} \right) \frac{(V_{\parallel} - v_{\parallel}) \exp \left(-\frac{v_{\perp}^2}{2\Delta_{\perp}^2} - \frac{v_{\parallel}^2}{2\Delta_{\parallel}^2} \right)}{\left((V_{\parallel} - v_{\parallel})^2 + (V_{\perp} - v_{\perp} \cos \varphi)^2 + v_{\perp}^2 \sin^2 \varphi \right)^{3/2}} v_{\perp} d\varphi dv_{\parallel} dv_{\perp}.$$

(1.12)

Within an accuracy of about 2% the upper limit of the integrals over velocity components can be replaced from infinity to three corresponding rms values and integration over φ can be performed from 0 to π due to symmetry of the formulae. In this case the friction force components can be calculated as:

$$\begin{aligned}
F_{\perp} &= -\frac{4\pi Z^2 e^4 n_e}{m \cdot \text{Int}} \int_0^{3\Delta_{\perp}} \int_{-3\Delta_{\parallel}}^{3\Delta_{\parallel}} \int_0^{\pi} \ln\left(\frac{\rho_{\max}}{\rho_{\min}}\right) \frac{(V_{\perp} - v_{\perp} \cos \varphi) \exp\left(-\frac{v_{\perp}^2}{2\Delta_{\perp}^2} - \frac{v_{\parallel}^2}{2\Delta_{\parallel}^2}\right)}{\left((V_{\parallel} - v_{\parallel})^2 + (V_{\perp} - v_{\perp} \cos \varphi)^2 + v_{\perp}^2 \sin^2 \varphi\right)^{3/2}} v_{\perp} d\varphi dv_{\parallel} dv_{\perp}, \\
F_{\parallel} &= -\frac{4\pi Z^2 e^4 n_e}{m \cdot \text{Int}} \int_0^{3\Delta_{\perp}} \int_{-3\Delta_{\parallel}}^{3\Delta_{\parallel}} \int_0^{\pi} \ln\left(\frac{\rho_{\max}}{\rho_{\min}}\right) \frac{(V_{\parallel} - v_{\parallel}) \exp\left(-\frac{v_{\perp}^2}{2\Delta_{\perp}^2} - \frac{v_{\parallel}^2}{2\Delta_{\parallel}^2}\right)}{\left((V_{\parallel} - v_{\parallel})^2 + (V_{\perp} - v_{\perp} \cos \varphi)^2 + v_{\perp}^2 \sin^2 \varphi\right)^{3/2}} v_{\perp} d\varphi dv_{\parallel} dv_{\perp},
\end{aligned}
\tag{1.13}$$

where the normalization factor is calculated in accordance with:

$$\text{Int} = \int_0^{3\Delta_{\perp}} \int_{-3\Delta_{\parallel}}^{3\Delta_{\parallel}} \int_0^{\pi} \exp\left(-\frac{v_{\perp}^2}{2\Delta_{\perp}^2} - \frac{v_{\parallel}^2}{2\Delta_{\parallel}^2}\right) v_{\perp} d\varphi dv_{\parallel} dv_{\perp}. \tag{1.14}$$

The minimal impact parameter is the following function of the electron velocity components:

$$\rho_{\min} = \frac{Ze^2}{m_e} \frac{1}{(V_{\parallel} - v_{\parallel})^2 + (V_{\perp} - v_{\perp} \cos \varphi)^2 + v_{\perp}^2 \sin^2 \varphi}. \tag{1.15}$$

At the ion velocity $V \gg \Delta_{\parallel}, \Delta_{\perp}$ the minimal impact parameter becomes to be constant:

$$\rho_{\min} = \frac{Ze^2}{m_e} \frac{1}{V_{\perp}^2 + V_{\parallel}^2}, \tag{1.16}$$

and Coulomb logarithm can be removed from the integral. At extremely small ion velocity the calculation of the minimal impact parameter in accordance with the formula (1.16) leads to zero friction force value, when becomes to be $\rho_{\min} > \rho_{\max}$. One can avoid this problem introducing mean minimal impact parameter in accordance with

$$\rho_{\min} = \frac{Ze^2}{m_e} \frac{1}{V_{\perp}^2 + V_{\parallel}^2 + \Delta_{\perp}^2 + \Delta_{\parallel}^2}. \tag{1.17}$$

When the Coulomb logarithm L_C is constant the two of three integrals in (1.12) can be calculated analytically and the friction force components can be written in accordance with Binney's formulae:

$$\begin{aligned}
F_{\perp} &= 2\sqrt{2\pi} \frac{n_e e^4 Z^2 L_C}{m} \frac{V_{\perp}}{\Delta_{\perp}^3} B_{\perp} \\
F_{\parallel} &= 2\sqrt{2\pi} \frac{n_e e^4 Z^2 L_C}{m} \frac{V_{\parallel}}{\Delta_{\perp}^3} B_{\parallel},
\end{aligned} \tag{1.19}$$

where B_{\perp} and B_{\parallel} are the following integrals:

$$\begin{aligned}
B_{\perp} &= \int_0^{\infty} \frac{\exp\left(-\frac{V_{\perp}^2}{2\Delta_{\perp}^2} \frac{1}{1+q} - \frac{V_{\parallel}^2}{2\Delta_{\perp}^2} \frac{1}{(\Delta_{\parallel}/\Delta_{\perp})^2 + q}\right)}{(1+q)^2 \left((\Delta_{\parallel}/\Delta_{\perp})^2 + q\right)^{1/2}} dq, \\
B_{\parallel} &= \int_0^{\infty} \frac{\exp\left(-\frac{V_{\perp}^2}{2\Delta_{\perp}^2} \frac{1}{1+q} - \frac{V_{\parallel}^2}{2\Delta_{\perp}^2} \frac{1}{(\Delta_{\parallel}/\Delta_{\perp})^2 + q}\right)}{(1+q) \left((\Delta_{\parallel}/\Delta_{\perp})^2 + q\right)^{3/2}} dq.
\end{aligned} \tag{1.20}$$

In the case of uniform Maxwellian distribution (when $\Delta_{\parallel} = \Delta_{\perp} = \Delta_e$) the integrals (1.20) coincide with each other and reproduce Chandrasekhar's formula. In Budker's notation it has the following form:

$$\begin{aligned}
\vec{F} &= -\frac{\vec{V}}{V^3} \frac{4\pi m_e e^4 Z^2 L_C}{m} \varphi\left(\frac{V}{\Delta_e}\right), \text{ where} \\
\varphi(x) &= \sqrt{\frac{2}{\pi}} \int_0^x e^{-y^2/2} dy - \sqrt{\frac{2}{\pi}} x e^{-x^2/2}.
\end{aligned} \tag{1.21}$$

The formulae (1.12) have to give the same result when the logarithm is removed from the integrals.

1.2. Asymptotic representation

For fast simulation of the cooling process in the BETACOOOL were used asymptotic formulae derived by I. Meshkov. In the case, when transverse velocity spread of electrons is substantially larger than longitudinal one the friction force components are approximated in three ranges of the ion velocity.

I. High velocity $V \geq \Delta_{\perp}$, here longitudinal and transverse components of the friction force are equal:

$$\vec{F} = -\frac{4\pi Z^2 e^4 n_e L_C}{m} \frac{\vec{V}}{V^3}, \tag{1.22}$$

and in this range the friction force shape coincides with formula (1.21).

II. Low velocity $\Delta_{\parallel} \leq V < \Delta_{\perp}$. Here the transverse component of the friction force is given by the following expression:

$$F_{\perp} = -\frac{4\pi Z^2 e^4 n_e L_C}{m} \cdot \frac{V_{\perp}}{\Delta_{\perp}^3}, \tag{1.23}$$

and longitudinal one:

$$F_{\parallel} = -\frac{4\pi Z^2 e^4 n_e L_C}{m} \frac{V_{\parallel}}{|V_{\parallel}| \Delta_{\perp}^2}. \tag{1.24}$$

III. Superlow velocity $V < \Delta_{\parallel}$. Here the transverse component of the friction force is equal to zero, the longitudinal component is given by:

$$F_{\parallel} = -\frac{4\pi Z^2 e^4 n_e L_C}{m} \frac{V_{\parallel}}{\Delta_{\parallel} \Delta_{\perp}^2}. \quad (1.25)$$

The minimal impact parameter in the Coulomb logarithm is equal to:

$$\rho_{\min} = \frac{Ze^2}{m} \frac{1}{V^2 + \Delta_e^2}. \quad (1.26)$$

For the longitudinal component of the friction force at zero transverse velocity the asymptotic formulae was derived by Ya. Derbenev in the following form:

$$F_{\parallel} = -\frac{4\pi Z^2 e^4 n_e L(V_{\parallel})}{m} \frac{V_{\parallel}}{\Delta_{\parallel} \Delta_{\perp}^2} \sqrt{\frac{2}{\pi}}, \text{ if } V \ll \Delta_{\parallel}. \quad (1.27)$$

$$F_{\parallel} = -\frac{4\pi Z^2 e^4 n_e}{m} \left[L(V_{\parallel}) \frac{V_{\parallel}}{|V_{\parallel}| \Delta_{\perp}^2} - \sqrt{\frac{\pi}{2}} L(\Delta_{\perp}) \frac{V_{\parallel}}{\Delta_{\perp}^3} \right], \text{ if } \Delta_{\perp} > V \gg \Delta_{\parallel}. \quad (1.28)$$

Here the Coulomb logarithms are calculated in accordance with the following formulae:

$$L(V_{\parallel}) = \ln \left(\frac{\sqrt{V_{\parallel}^2 m}}{\sqrt{4\pi n_e e^2}} / \rho_{\min} \right), \quad (1.29)$$

$$L(\Delta_{\perp}) = \ln \left(\frac{\sqrt{\Delta_{\perp}^2 m}}{\sqrt{4\pi n_e e^2}} / \rho_{\min} \right). \quad (1.30)$$

In order to provide uniform usage of the formulae in the program the friction force calculation was realized in three ranges of the ion velocity similarly to Meshko's asymptotes.

I. High velocity $V \geq \Delta_{\perp}$, here longitudinal and transverse components of the friction force are equal:

$$F_{\perp} = -\frac{4\pi Z^2 e^4 n_e L_C}{m} \frac{V_{\perp}}{V^3}, \quad (1.31)$$

$$F_{\parallel} = -\frac{4\pi Z^2 e^4 n_e}{m} \left(L_C \frac{V_{\parallel}}{V^3} - \sqrt{\frac{2}{\pi}} L(\Delta_{\perp}) \frac{1}{V_{\parallel}^2} \right). \quad (1.32)$$

II. Low velocity $\Delta_{\parallel} \leq V < \Delta_{\perp}$. Here the transverse component of the friction force is given by the following expression:

$$F_{\perp} = -\frac{4\pi Z^2 e^4 n_e L_C}{m} \frac{V_{\perp}}{\Delta_{\perp}^3}, \quad (1.33)$$

and longitudinal one:

$$F_{\parallel} = -\frac{4\pi Z^2 e^4 n_e}{m} \left(L_c \frac{V_{\parallel}}{\sqrt{V_{\parallel}^2 + \Delta_{\parallel}^2 \Delta_{\perp}^2}} - \sqrt{\frac{2}{\pi}} L(\Delta_{\perp}) \frac{V_{\parallel}}{\Delta_{\perp}^3} \right). \quad (1.34)$$

III. Superlow velocity $V < \Delta_{\parallel}$. Here the transverse component of the friction force is equal to zero, the longitudinal component is given by:

$$F_{\parallel} = -\frac{4\pi Z^2 e^4 n_e}{m} L_c \frac{V_{\parallel}}{\sqrt{V_{\parallel}^2 + \Delta_{\parallel}^2 \Delta_{\perp}^2}}. \quad (1.35)$$

These formulae in the case $V_{\perp} = 0$ give the correct result for longitudinal component of the friction force (1.27), (1.28) and have a correct asymptotes at high ion velocity. The transverse component of the force is calculated in accordance with Meshkov's representation.

1.3. Benchmarking the code

All the formulae for the numerical friction force calculation (1.12, 1.19 and 1.21) have to coincide in the case of uniform Maxwellian distribution of the electrons if the Coulomb logarithm is moved under the integral. In this case the friction is symmetrical in the transverse and longitudinal degrees of freedom. The formulae were tested at Recycler cooling system parameters that are listed in the Table 1.1.

Table 1. The cooling system parameters used in simulations.

Cooling section length, m	20
Electron energy, MeV	4.36
Beta functions in the cooling section, m	20
Electron current, A	0.2
Electron beam radius, cm	0.45
Transverse temperature, eV	0.5
Longitudinal temperature, eV	0.01

In the Fig. 1.1. the results of the calculations at $T_{\parallel} = T_{\perp} = 0.5$ eV using different formulae are presented.

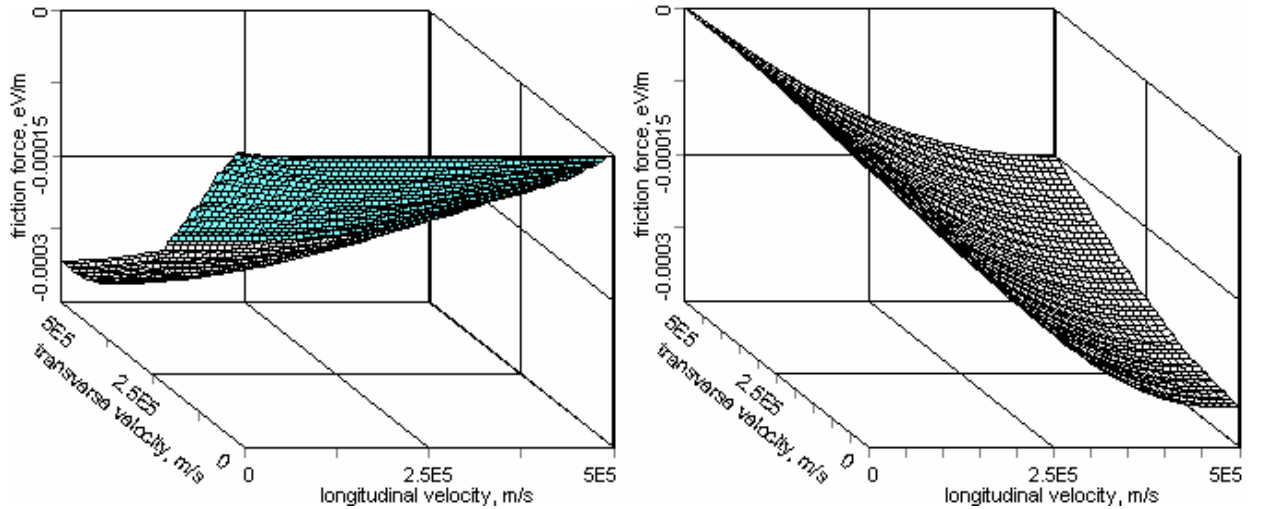


Fig. 1.1, a. Friction force components (left plot - transverse, right plot – longitudinal) as functions of the ion velocity calculated with Chandrasekhar's formula.

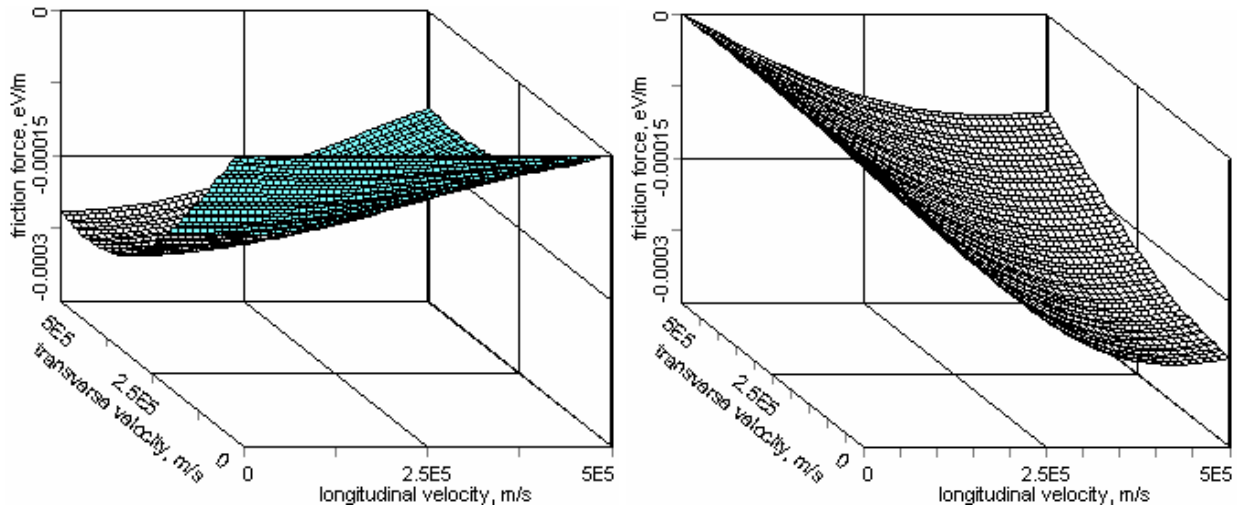


Fig. 1.1, b. Friction force components (left plot - transverse, right plot – longitudinal) as functions of the ion velocity calculated with Binney's formula. Integration step is 0.003, upper limit is 3.

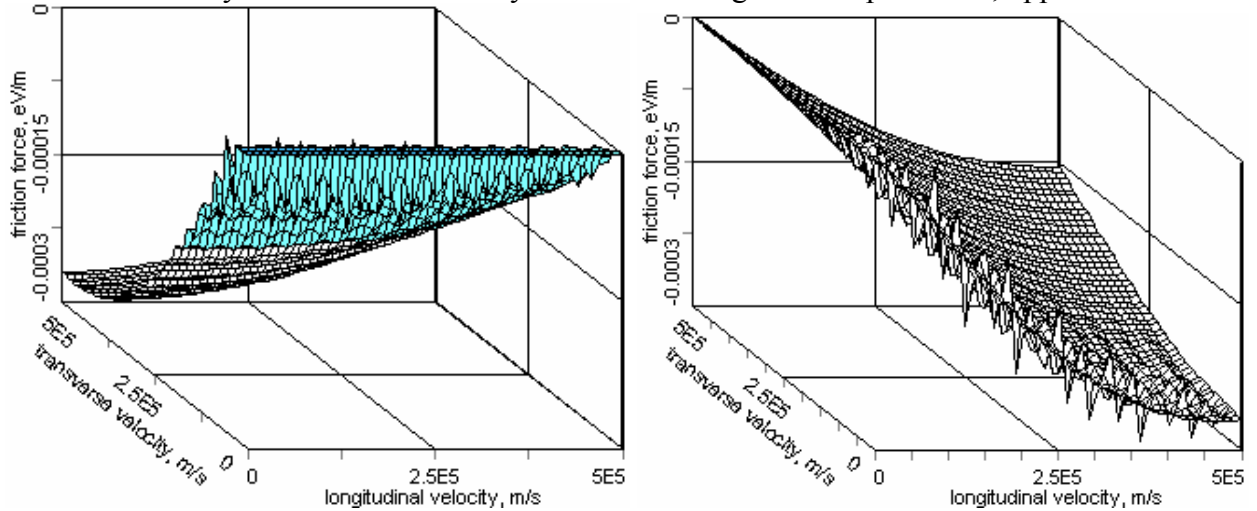


Fig. 1.1, c. Friction force components (left plot - transverse, right plot – longitudinal) as functions of the ion velocity calculated by numerical evaluation of 3D integral (1.13). The Coulomb logarithm is removed from the integral. Number of integration steps over the transverse velocity is 27, over the longitudinal velocity - 26, over the angle - 15.

The maximum position and amplitude of the friction force calculated using different formulae coincide within the accuracy of numerical integration. The numerical evaluation of 3D integral requires by about 100 times longer calculation time and the accuracy decreases in the region of small velocity (one can see a numerical noise in the Fig. 1.1, b due to small number of the integration steps). The numerical noise in the region of small ion velocity at evaluation of 3D integral is sufficiently less, when the Coulomb logarithm is kept under the integral.

At flattened electron velocity distribution the Binney's formula has to coincide with the numerical evaluation of 3D integral (1.13) when the Coulomb logarithm is removed over the integral. In the Fig 1.2 the results of the force calculation at $T_{\parallel} = 0.01$ eV are presented. At the flattened velocity distribution the amplitude of the longitudinal component of the friction force is larger than the transverse one, and the maximum position is located near the electron longitudinal velocity spread. Both the formulae give the same result with the accuracy of numerical integration.

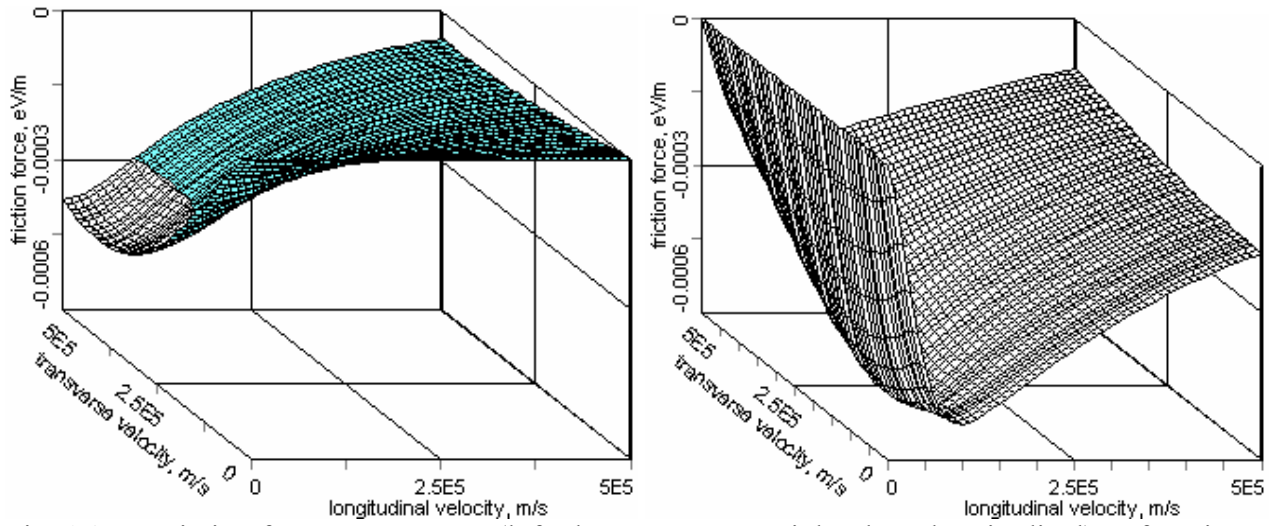


Fig. 1.2, a. Friction force components (left plot - transverse, right plot – longitudinal) as functions of the ion velocity calculated with Biney's formula. Integration step is 0.003, upper limit is 3.

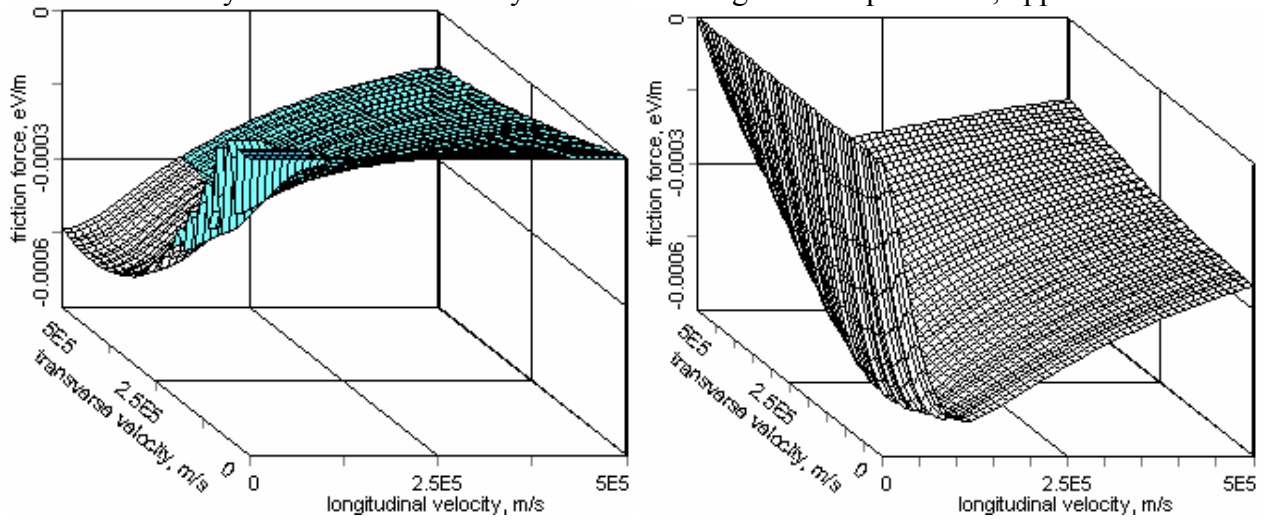


Fig. 1.2, b. Friction force components (left plot - transverse, right plot – longitudinal) as functions of the ion velocity calculated by numerical evaluation of 3D integral (1.13). The Coulomb logarithm is removed from the integral. Number of integration steps over the transverse velocity is 27, over the longitudinal velocity - 26, over the angle - 15.

The difference in the friction forces calculated as a 3D integral with Coulomb logarithm inside or outside the integral is illustrated in the Fig. 1.3.

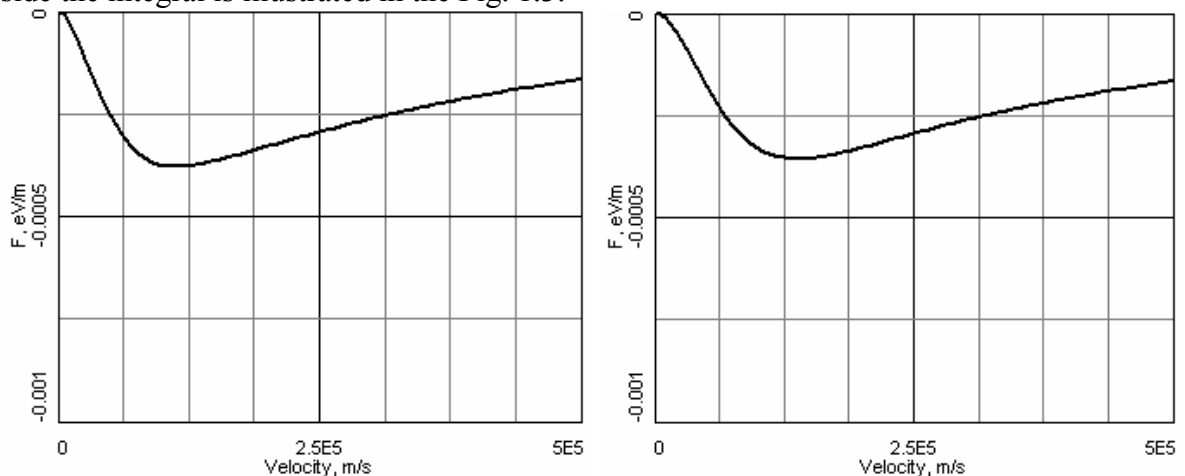


Fig. 1.3. The longitudinal component of the friction force as function of longitudinal ion velocity. Coulomb logarithm is removed from the integral - left plot, Coulomb logarithm is under the integral – right plot.

One can see that the accurate treatment of the Coulomb logarithm leads to slight decrease of the friction force value and displacement of the maximum position into the region of larger ion velocity. It means that at used parameters of the cooler the Binney's formula provide good enough accuracy of the calculation at sufficiently less calculation time. At other cooler parameters the numerical evaluation of 3D integral can be used for estimation of the accuracy of other formulae and for simulations can be used more fast algorithm.

For comparison between numerical and asymptotic representations of the friction force the longitudinal component of the force calculated in accordance with Meshkov's formulae is shown in the Fig. 1.4. One can see that this asymptote sufficiently overestimate the friction force and it can be used only for very rough estimates.

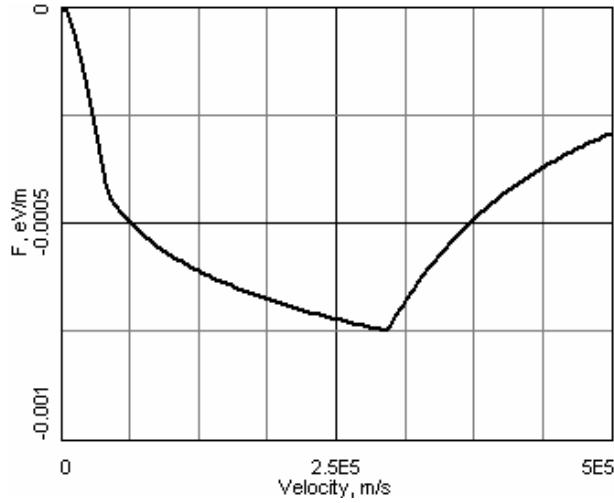


Fig. 1.4. Meshkov's asymptote of the friction force longitudinal component.

More appropriate candidate for comparison of the numerical results of the friction force calculation with experiments is Recycler cooling system realizing the nonmagnetized cooling of antiprotons. To simplify the comparison a few modifications in the program were done.

2. Modeling of Recycler cooling system

At usual electron cooling systems a longitudinal magnetic field is used for transportation of the electron beam. At decrease of the magnetic field value in a cooling section the beam quality fast decreases and investigation of nonmagnetized regime of the electron cooling can not be provided in well controlled conditions. In July 2005 the Recycler cooling system was put into operation in Fermilab. At this cooling system the longitudinal magnetic field in the cooling section is used only to preserve angular spread of electrons θ at the level below $200 \mu\text{rad}$. The required longitudinal magnetic field value B is 105 G that corresponds to electron rotation with Larmor radius

$$\rho_{\perp} = \frac{pc}{eB} \theta \approx 3 \cdot 10^{-4} m,$$

where $pc = 4,85 \text{ MeV}$ is the electron momentum. The cooling section length is 20 m which approximately corresponds to 2 steps of the Larmor helix. Maximum impact parameter at maximum electron current of 500 mA is restricted by time of flight the cooling section and it is equal

$$\rho_{\text{max}} \approx 7 \cdot 10^{-5} m,$$

that is smaller than the electron Larmor radius. At such parameters one can expect, that the impact of magnetized collisions into the friction force is negligible.

To provide accurate comparison between results of experimental investigations at Recycler and numerical simulation with BETACOOOL a few new algorithms were implemented and tested. General method for friction force measurements at Recycler is Voltage Step method and general attention was devoted to simulation of this procedure in BETACOOOL.

One of the peculiarities of the Recycler cooling system is sufficient dependence of the electron transverse velocity spread on the distance from the beam centre. This effect appears due to the beam envelope mismatch with the transportation channel. In the first approximation this effect can be presented as a linear increase of the velocity spread with radial co-ordinate:

$$\Delta_{\perp} = \frac{d\Delta_{\perp}}{dr} r, \quad (2.1)$$

where the velocity gradient $\frac{d\Delta_{\perp}}{dr}$ is input into the simulations as an additional parameter of the electron beam (last parameter in the Fig. 2.1).

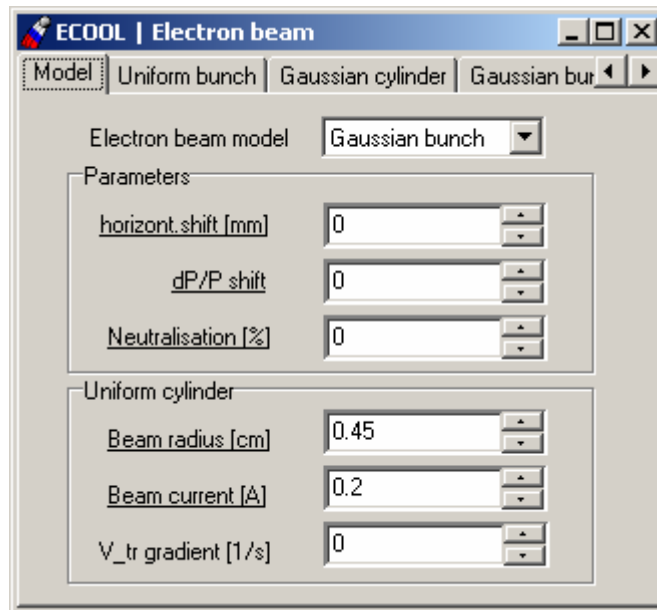


Fig. 2.1. Modification of the visual form for input a transverse velocity gradient.

To simulate the High Voltage step in the electron cooler the electron momentum can be varied during simulations by change of the parameter “dP/P shift” (Fig. 2.1). RMS dynamics simulation presumes that the mean ion momentum is constant during evolution therefore the voltage step method can be simulated only in the frame of Model Beam algorithm. The mean momentum of the ions is output in additional curve “dpmo2t.cur” and can be visualized in the same plot with a momentum spread in the corresponding form of the Windows interface.

An example of the cooling process simulation is presented in the Fig. 2.2. The red curve correspond to mean antiproton momentum. The first 1700 sec correspond to preliminary cooling of antiprotons. At 1700 sec the electron momentum was shifted by the relative value of 10^{-3} and during next 2000 sec the mean antiproton momentum is cooled to the new momentum of the electrons. The green curve presents the variation in time of the antiproton momentum spread.

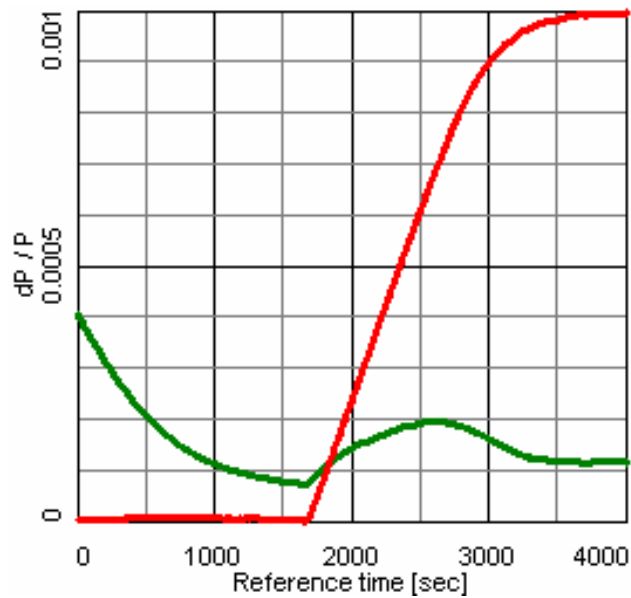


Fig. 2.2. Simulation of the voltage step method using BETACOOOL program. The electron beam parameters are presented in the Table 1.1.

Evolution of the antiproton momentum during the friction force measurement is also output as a 3D plot of the profile versus time as shown in the Fig 2.3.

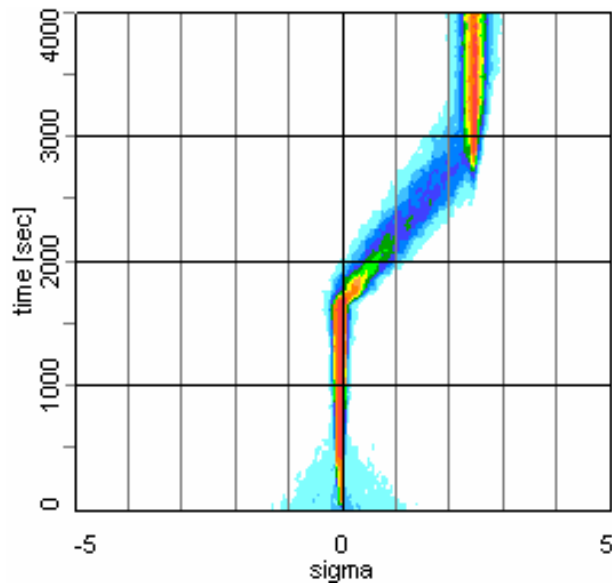


Fig. 2.3. The longitudinal profile evolution during friction force measurement.

To reproduce the procedure using in Fermilab for the beam longitudinal distribution measurement the possibility to average of a few consequent longitudinal profiles was introduced. An example of a few consequent averaged profiles calculated with BETACOOOL after 2 keV step of the electron energy is presented in the Fig. 2.4. The electron beam current is 500 mA.

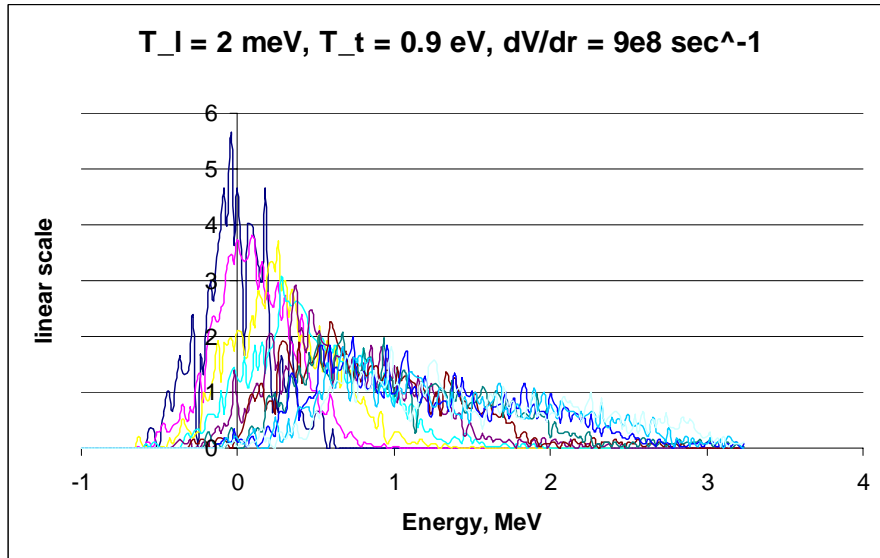


Fig. 2.4. Evolution of the longitudinal profile in time. Distance between slices is 50 sec.

3. Stochastic cooling simulation

3.1. Stochastic cooling in accordance to H.Stochorst model

Algorithm for stochastic cooling simulation was implemented into BETACOOOL in accordance to the model derived by H.Stochorst (FZJ). The stochastic cooling for transverse degrees of freedom is simulated under assumption that the quarter wave loop pickup and kicker are located in the ring at positions with zero dispersion and its derivative. The phase advance of the betatron oscillations from pickup to kicker assumed to be $(2k+1)\frac{\pi}{2}$, where k is integer, and the phase errors are minimized. For two transverse degrees of freedom there is no band overlap. Cooling of longitudinal degree of freedom is simulated in accordance with the theory of filter method. The simulation presumes that the longitudinal cooling is applied using analogous system components as in the case for transverse cooling. Pickup and kicker are then operated in Σ -mode and the signal pass contains a notch filter that provides the necessary information on the energy deviation of a particle for the coherent signal. Simultaneously the filter rejects the noise signals at frequency near the revolution harmonics.

The model permits to estimate characteristic cooling times, consumption power and generate a kick of the particle momentum in the Model Beam algorithm using geometry parameters of pickup and kicker electrodes

3.1.1. Cooling rate calculation

The transverse emittance derivative over time in each plane can be written in the following form:

$$\frac{d\varepsilon}{dt} = -\frac{1}{\tau_{cool}}(\varepsilon - \varepsilon_{\infty}), \quad (3.1.1)$$

where τ_{cool} describes the drift term in the Fokker-Plank equation and the equilibrium emittance ε_{∞} corresponds to the diffusion term [3, 4]. The characteristic time of the emittance variation due to action of the stochastic cooling is equal:

$$\frac{1}{\tau} = \frac{1}{\varepsilon} \frac{d\varepsilon}{dt} = -\frac{1}{\tau_{cool}} \frac{\varepsilon - \varepsilon_{\infty}}{\varepsilon}. \quad (3.1.2)$$

The transverse cooling time is determined from the parameters of the cooling system as follows:

$$\frac{1}{\tau_{cool}} = \frac{16}{3} \frac{|\eta| \delta W^2}{N f_0} \cdot x J(x). \quad (3.1.3)$$

Here $\eta = \frac{1}{\gamma^2} - \frac{1}{\gamma_{tr}^2}$ is off-momentum factor of the storage ring, γ is Lorenz factor of the ion, γ_{tr} is critical energy of the ring in the rest energy units. f_0 is the ion revolution frequency. $W = f_{max} - f_{min}$ is the bandwidth of the system with lower frequency f_{min} and upper frequency f_{max} . N is the ion number. Total momentum spread of the beam δ is calculated from r.m.s. value in accordance with the shape of distribution function. For instance, at a parabolic distribution

$$\delta = 4 \frac{\Delta p}{p_{rms}}. \quad (3.1.4)$$

Formfactor $xJ(x)$ is calculated through a frequency range as follows:

$$xJ(x) = x \left(1 - 2x \ln \left(\frac{x + f_{max}/W}{x + f_{min}/W} \right) + \frac{x^2}{(x + f_{max}/W)(x + f_{min}/W)} \right). \quad (3.1.5)$$

The x value is proportional to the linear gain of the system from pickup to kicker G_A :

$$x = G_A / R, \quad (3.1.6)$$

where the coefficient R is determined by parameters of pickup and kicker:

$$R = \frac{16}{3A_2} \frac{|\eta| \delta W}{N} \frac{1}{Z} \frac{h_p h_k}{\sigma_p \sigma_k} \frac{1}{\sqrt{\beta_p \beta_k n_p n_k}} \frac{\beta p c}{(1 + \beta) e^2 f_0^2 l_{loop}}. \quad (3.1.7)$$

Here $h_{p,k}$ is height of the gap at pickup and kicker, the pickup and kicker sensitivity are given by

$$\sigma_{p,k} = 2 \tanh \left(\frac{\pi w_{p,k}}{2h_{p,k}} \right), \quad (3.1.8)$$

where $w_{p,k}$ is the electrode width, Z – characteristic impedance, $\beta_{p,k}$ – beta functions in the pickup and kicker position, $n_{p,k}$ is the number of lambda quarter loops in pickup and kicker, l_{loop} is the loop length. βc , p and e – are the ion velocity, momentum and charge correspondingly, c is the speed of light. Value A_1 is calculated through the bandwidth as follows

$$A_1 = \frac{1}{W} \int_{f_{min}}^{f_{max}} \sin^2 \left(\frac{2\pi f l_{loop}}{\beta c} \right) df. \quad (3.1.9)$$

The equilibrium emittance value is determined by the cooling system parameters and the thermal noise power:

$$\varepsilon_\infty = \frac{1}{4} \frac{A_3}{A_2} \sqrt{\frac{\beta_k n_k}{\beta_p n_p}} (T_A + T_R) \frac{h_p \sigma_k}{h_k \sigma_p} l_{loop} \frac{1 + \beta}{\beta p c} G_A, \quad (3.1.10)$$

wher T_A and T_R are the pickup and preamplifier temperatures correspondingly. The values A_2 and A_3 are the following integrals:

$$A_2 = \frac{1}{W} \int_{f_{\min}}^{f_{\max}} \frac{\sin^2(2\pi f l_{loop} / \beta c)}{2\pi f l_{loop} / \beta c} df, \quad (3.1.11)$$

$$A_3 = \frac{1}{W} \int_{f_{\min}}^{f_{\max}} \left(\frac{\sin(2\pi f l_{loop} / \beta c)}{2\pi f l_{loop} / \beta c} \right)^2 df. \quad (3.1.12)$$

For longitudinal degree of freedom the cooling time calculation is based on solution of Fokker-Plank equation. The ion distribution in the energy space is described by the function $\Psi(E)$, where E is the energy deviation from mean kinetic energy E_0 . The Fokker-Plank equation for the distribution function $\Psi(E,t)$, which describes the particle density in the energy space, has the following form

$$\frac{\partial}{\partial t} \Psi(E,t) = -\frac{\partial}{\partial E} \left[F(E)\Psi(E,t) - D(E,t) \frac{\partial}{\partial E} \Psi(E,t) \right],$$

where E is energy deviation from the mean kinetic energy E_0 .

Drift term in this equation describes the coherent cooling

$$F(E) = \frac{E}{\tau_0},$$

where τ_0 is the ‘‘single particle’’ cooling time. The diffusion term contains two parts

$$D(E,t) = D_{th}(E,t) + D_s(E,t)$$

the beam heating due to thermal noise

$$D_{th}(E,t) = AE^2$$

and beam heating due to the finite Schottky noise density

$$D_s(E,t) = BE^2\Psi(E,t).$$

To calculate dynamics of the rms beam parameters the Fokker-Plank equation can be reduced to equation for the second moment of the distribution function which is determined by

$$\sigma_E^2 = \frac{1}{N} \int E^2 \Psi(E) dE \quad (3.1.13)$$

This equation has the following form [5, 4]:

$$\frac{d\sigma_E^2}{dt} = -\frac{2}{\tau_0}\sigma_E^2 + A\sigma_E^2 + \frac{3B}{N} \int E^2 \Psi^2(E,t) dE$$

Rms dynamics algorithm presumes Gaussian distribution in all degrees of freedom. In the energy space it corresponds to the density $\rho(E,t) = \frac{1}{N} \Psi(E,t)$ given by

$$\rho = \frac{1}{\sqrt{2\pi}\sigma_E} \exp\left(-\frac{(E-E_0)^2}{2\sigma_E^2}\right)$$

Thus the integral in the last term is equal to

$$\int E^2 \Psi^2 dE = N^2 \int E^2 \rho^2 dE = \frac{N^2 \sigma_E}{4\sqrt{\pi}},$$

and evolution of the second order momentum of the distribution function is described by the following equation

$$\frac{d\sigma_E^2}{dt} = -\frac{2}{\tau_{cool}}\sigma_E^2 + \frac{3B}{4\sqrt{\pi}} N \sigma_E, \quad (3.1.14)$$

The values A , B , τ_{cool} and τ_0 are determined from the cooling system parameters as follows:

$$\frac{1}{\tau_{cool}} = \frac{1}{\tau_0} - 3A, \quad (3.1.15)$$

$$A = e^2 (T_R + T_A) Z n_k \left(\frac{\kappa}{E_0}\right)^2 G_A^2 \frac{W}{f_0} \left(f_C^2 + \frac{W^2}{12}\right), \quad (3.1.16)$$

$$B = A_1 e^4 n_k n_p Z^2 \frac{|\kappa|}{E_0} G_A^2 f_0 f_C W, \quad (3.1.17)$$

the ‘‘single particle’’ cooling time τ_0 is given by

$$\frac{1}{\tau_0} = 2A_1 e^2 \sqrt{n_p n_k} Z G_A W f_C \frac{\kappa}{E_0}, \quad (3.1.18)$$

where $\kappa = \eta \frac{\gamma}{\gamma+1}$, $f_C = \frac{f_{\min} + f_{\max}}{2}$ is the central frequency of the band. A_1 is determined by the formula (3.1.9) at the loop length of the longitudinal electrodes.

Characteristic rate for the longitudinal emittance deviation (in Betacool for the longitudinal emittance such a definition $\varepsilon_{long} = \left(\frac{\Delta p}{p}\right)^2$ is used) can be calculated in accordance with

$$\frac{1}{\tau} = \frac{1}{\varepsilon_{long}} \frac{d\varepsilon_{long}}{dt} = \frac{1}{\sigma_E^2} \frac{d\sigma_E^2}{dt} = -\frac{2}{\tau} + \frac{3BN}{4\sqrt{\pi}\sigma_E}. \quad (3.1.19)$$

Using relation between energy and momentum deviations $\frac{\sigma_E}{E_0} = \frac{1+\gamma}{\gamma} \frac{\Delta p}{p}$ the last equation can be reduced to:

$$\frac{1}{\tau} = -\frac{2}{\tau_{cool}} + \frac{3BN\gamma}{4\sqrt{\pi}\sqrt{\varepsilon_{long}}E_0(1+\gamma)}. \quad (3.1.20)$$

3.1.2. Power consumption

Optimization of the cooling system parameters presumes not only minimization of the equilibrium emittance and cooling time, but also keeping a consumption power in a reasonable range. The consumption power for transverse cooling chain is calculated as a sum of thermal noise power and Schottky power. The thermal noise power in the cooling bandwidth is given by:

$$P_{th} = (T_A + T_R)G_A^2W, \quad (3.1.21)$$

and this value has to be corrected to take into account losses in combiner P_{comb} :

$$P_{th,tot} = P_{th} \cdot 10^{P_{comb}[dB]/10} \quad (3.1.22)$$

The Schottky power in the cooling band is

$$P_S = A_1 N n_p \beta_p Z \left(\frac{\sigma_p}{h_p} \right)^2 e^2 f_0 \varepsilon_{rms} G_A^2 W. \quad (3.1.23)$$

The total power is calculated as the sum of (3.1.22) and (3.1.23) plus losses in an electronic chain. The losses in the electronic chain are input into program as additional parameter P_{loss} and total consumption power is calculated in accordance with:

$$P_{tot} = (P_{th,tot} + P_S) \cdot 10^{P_{loss}[dB]/10}. \quad (3.1.24)$$

The loss power includes losses in splitter, reserve noise signal and others losses and by the order of magnitude is about 10 dB.

The filtered thermal noise power in the cooling bandwidth at the kicker input can be estimated from:

$$P_{th} = \frac{1}{3}(T_A + T_R)G_A^2W. \quad (3.1.25)$$

The filtered Schottky power at the kicker input is

$$P_S = 4A_1 N n_p Z e^2 G_A^2 \eta^2 \left(\frac{\Delta p}{p} \right)_{rms}^2 \frac{W}{f_0} \left(f_C^2 + \frac{W^2}{12} \right). \quad (3.1.26)$$

The total power consumption is calculated by the same way as for transverse degrees of freedom.

3.1.3. Kick of the ion momentum components due to action of stochastic cooling

In the frame of Model Beam algorithm each particle is presented as a 6 co-ordinate vector:

$\vec{X} = \left(x, \frac{p_x}{p}, y, \frac{p_y}{p}, s - s_0, \frac{\Delta p}{p} \right)$, where x and y are the horizontal and vertical co-ordinates, p_x and p_y are corresponding momentum components, $s - s_0$ is the distance from the bunch center (in the case of coasting beam this variable can have arbitrary value), Δp is the particle momentum deviation from momentum of reference particle p .

Some effects like electron cooling or internal target are located in some fixed points of the ring. Such effects are characterizing by the ring lattice functions in the effect position. Some effects like intrabeam scattering or scattering on residual gas are distributed over the total ring circumference. Average action of such effects can be applied to the beam in “averaged” position in the ring, that has the beta and dispersion functions equal to averaged over the ring ones, the alpha-functions and dispersion derivative are equal to zero. Between the effect position the particle co-ordinates are transformed using linear matrix at random phase advance (the random generation of the phase advance reflects that the integration step over time is sufficiently longer than revolution period and than betatron oscillation period). Action of each effect is simulated as the particle momentum variation in accordance with Langevin equation:

$$\left(p_{x,y,s} / p \right)_{fin} = \left(p_{x,y,s} / p \right)_{in} + \Lambda_{x,y,s} \Delta T + \sqrt{D_{x,y,s} \Delta T} \xi_{x,y,s}, \quad (3.1.27)$$

where p_s is the particle longitudinal momentum deviation, subscript *in* correspond to initial momentum value, subscript *fin* relates to final particle momentum after action of the effect, Λ and D are the drift and diffusion terms for corresponding degree of freedom, ΔT is step of the integration over time, ξ is Gaussian random number at unit dispersion. The regular variation of the particle momentum due to action of drift term can be rewritten as

$$\left(p_{x,y,s} / p \right)_{fin} = \left(p_{x,y,s} / p \right)_{in} \left(1 + \frac{\Lambda_{x,y,s}}{\left(p_{x,y,s} / p \right)_{in}} \Delta T \right). \quad (3.1.28)$$

Here the value $\frac{\Lambda_{x,y,s}}{\left(p_{x,y,s} / p \right)_{in}}$ does not depend on the effect poison in the ring, and it can be treated

as a “single-particle” cooling time. At large value of ΔT the absolute value of the term

$\frac{\Lambda_{x,y,s}}{\left(p_{x,y,s} / p \right)_{in}} \Delta T$ can be larger than unity (in the case of cooling this term has a negative sign). In

this case direct application of the formula (3.1.28) will lead to change a sign of corresponding momentum component and can lead also to increase of its absolute value. This situation corresponds to artificial diffusion heating of the beam on numerical algorithm. To avoid this

“numerical” diffusion at $\left| \frac{\Lambda_{x,y,s}}{\left(p_{x,y,s} / p \right)_{in}} \Delta T \right| > 1$ the formula (3.1.28) is transformed to the following

form

$$\left(p_{x,y,s} / p\right)_{fin} = \left(p_{x,y,s} / p\right)_{in} \times \exp\left\{\frac{\Lambda_{x,y,s}}{\left(p_{x,y,s} / p\right)_{in}} \Delta T\right\}, \quad (3.1.29)$$

which includes the (3.1.28) as a limit case at small ΔT .

In the case of random variation of the particle momentum components corresponding to diffusion term in (3.1.27) the kick has to be calculated tacking into account the ring lattice parameters in the effect position. In the simplest case at the constant diffusion the equation for the emittance variation in time can be written as follows:

$$\frac{d\varepsilon_{x,y}}{dt} = \frac{D_{x,y}}{2\varepsilon_{x,y}}, \quad (3.1.30)$$

that gives

$$\Delta\varepsilon_{x,y} = \frac{D_{x,y}}{2\varepsilon_{x,y}} \Delta T. \quad (3.1.31)$$

Tacking into account that rms momentum variation relates to the emittance variation as $\langle\theta^2\rangle = 2 \frac{\Delta\varepsilon_{x,y}}{\beta_{x,y}}$, for the momentum components variation we have:

$$\Delta\left(p_{x,y} / p\right) = \sqrt{\frac{D_{x,y}}{\varepsilon_{x,y} \beta_{x,y}} \Delta T \xi_{x,y}}, \quad (3.1.32)$$

where $\beta_{x,y}$ are the beta functions in the effect position in corresponding planes. For longitudinal degree of freedom emittance is determined as square of the rms momentum spread and at this definition we have:

$$\Delta(\Delta p / p) = \sqrt{k \frac{D_{long}}{2\varepsilon_{long}} \Delta T \xi}, \quad (3.1.33)$$

where $k = 1$ for coasting beam and $k = 2$ for bunched one.

For the transverse degree of freedom the drift term in (3.1.27) is calculated in accordance with the formula (2.3) for the “single particle” cooling time. The regular variation of transverse momentum component are calculated in accordance with (3.1.28, 3.1.29):

$$\left(p_{x,y} / p\right)_{fin} = \begin{cases} \left(p_{x,y} / p\right)_{in} \left(1 - \frac{\Delta T}{\tau_{cool,x,y}}\right), & \text{if } \left|\frac{\Delta T}{\tau_{cool,x,y}}\right| < 1 \\ \left(p_{x,y} / p\right)_{in} \exp\left(-\frac{\Delta T}{\tau_{cool,x,y}}\right), & \text{if } \left|\frac{\Delta T}{\tau_{cool,x,y}}\right| > 1 \end{cases} \quad (3.1.34)$$

Diffusion coefficient for the transverse degrees of freedom can be calculated using formula (3.1.10) for equilibrium emittance value. The emittance variation in time can be described by the following differential equation:

$$\frac{d\varepsilon_{x,y}}{dt} = -\frac{\varepsilon_{x,y}}{\tau_{cool,x,y}} + \frac{D_{x,y}}{2\varepsilon_{x,y}}. \quad (3.1.35)$$

From the other hand (3.1.1) gives

$$\frac{d\varepsilon_{x,y}}{dt} = -\frac{\varepsilon_{x,y}}{\tau_{cool,x,y}} + \frac{\varepsilon_{\infty,x,y}}{\tau_{cool,x,y}},$$

and for the diffusion coefficient we have:

$$D_{x,y} = \frac{2\varepsilon_{x,y}\varepsilon_{\infty,x,y}}{\tau_{cool,x,y}}. \quad (3.1.36)$$

The diffusion power is proportional to square of the linear gain G_A that can be seen from definitions of the cooling time and equilibrium emittance (3.1.3, 3.1.10). This result can be obtained directly from expression for emittance derivative before introduction of ε_{∞} as it done for instance in [3].

In accordance with (3.1.32) for the momentum components variation we have:

$$\Delta(p_{x,y}/p) = \sqrt{\frac{2\varepsilon_{\infty,x,y}}{\tau_{cool,x,y}\beta_{x,y}} \Delta T \xi_{x,y}}. \quad (3.1.37)$$

In the present version of the program the kick is applied to the ion momentum in “averaged” position of the ring.

For longitudinal degree of freedom the “single particle” cooling time τ_0 is given by (3.1.18), and the regular particle momentum variation is calculated as follows:

$$(\Delta p/p)_{fin} = \begin{cases} (\Delta p/p)_{in} \left(1 - k \frac{\Delta T}{\tau_0}\right), & \text{if } \left|\frac{\Delta T}{\tau_0}\right| < 1 \\ (\Delta p/p)_{in} \exp\left(-k \frac{\Delta T}{\tau_0}\right), & \text{if } \left|\frac{\Delta T}{\tau_0}\right| > 1 \end{cases} \quad (3.1.38)$$

At arbitrary distribution function the integral $\int E^2 \rho^2 dE$ can be estimated by the value $\frac{N^2 \sigma_E}{6}$, which is averaged for Gaussian and parabolic distributions. In this case the equation (3.1.14) can be rewritten as

$$\frac{d\sigma_E^2}{dt} = -\frac{2}{\tau_0} \sigma_E^2 + 3A\sigma_E^2 + \frac{B}{2} N\sigma_E$$

or taking into account that $\frac{\sigma_E}{E_0} = \frac{1+\gamma}{\gamma} \frac{\Delta p}{p}$ and $\varepsilon_{long} = \left(\frac{\Delta p}{p}\right)^2$

$$\frac{d\varepsilon_{long}}{dt} = -\frac{2}{\tau_0} \varepsilon_{long} + 3A\varepsilon_{long} + \frac{BN\gamma}{2E_0(\gamma+1)} \sqrt{\varepsilon_{long}}$$

The thermal and Shottky diffusion terms are independent, correspondingly the momentum kick due to diffusion is calculated as:

$$\Delta(\Delta p / p) = \sqrt{\left(\frac{BN\gamma}{2E_0(\gamma+1)}\right)^2 \varepsilon_{long} + (3A\varepsilon_{long})^2 k\Delta T \xi_s}. \quad (3.1.39)$$

Visual forms for input and output parameters of the stochastic cooling system are presented at the Fig. 3.1 – 3.3. Structure of the input file corresponds to the structure of interface part.

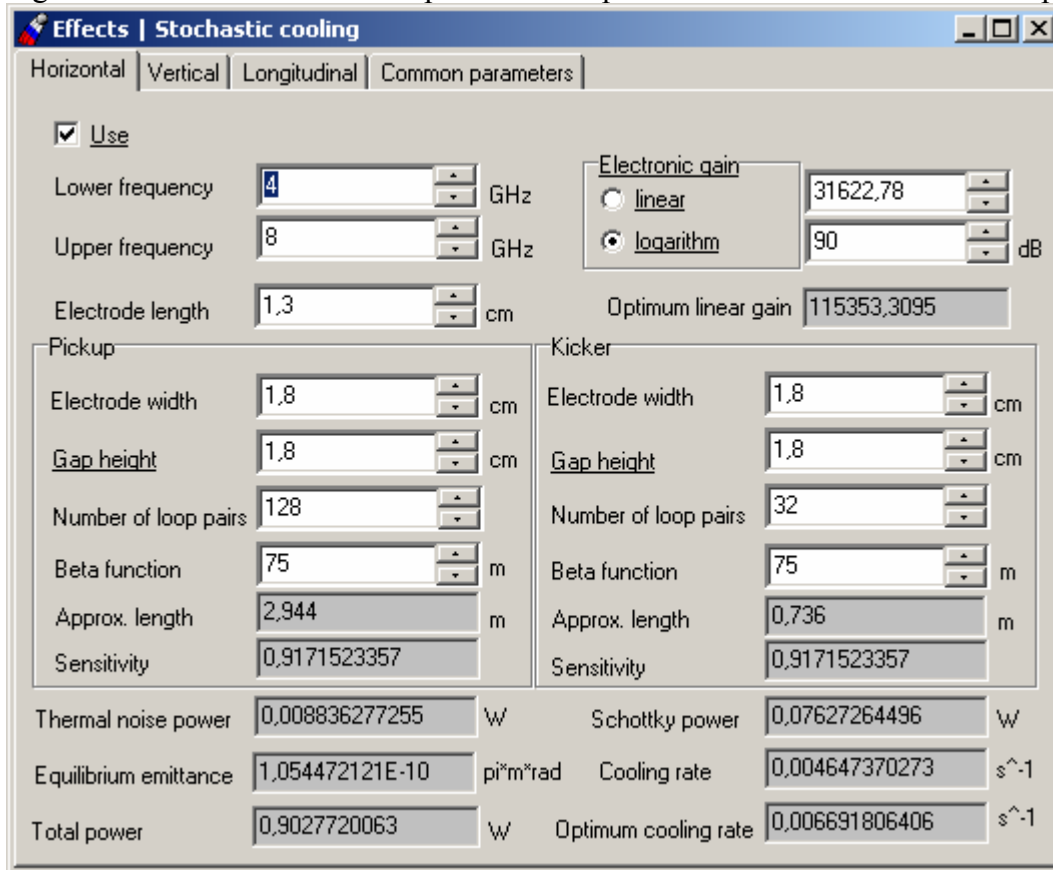


Fig. 3.1. Visual form for input and output parameters for transverse cooling chain.

Effects | Stochastic cooling

Horizontal | Vertical | Longitudinal | Common parameters

Use

Lower frequency GHz

Upper frequency GHz

Electrode length cm

Electronic gain

linear

logarithm dB

Optimum linear gain

Pickup number of loop pairs Approx length m

Kicker number of loop pairs Approx. length m

Thermal noise power W

Schottky power W

Total power W

Cooling rate s⁻¹ Optimum cooling rate s⁻¹

Equilibrium momentum spread

Fig. 3.2. Visual form for input and output parameters for longitudinal cooling chain.

Effects | Stochastic cooling

Horizontal | Vertical | Longitudinal | Common parameters

Total width of momentum distribution sigma

Pickup effective temperature K

Preamplifier temperature K

Characteristic impedance Ohm

Losses in combiner dB

Other losses dB

Fig. 3.3. Visual form for input parameters for power consumption calculation.

3.2. Optical stochastic cooling

Optical stochastic cooling (OSC) is proposed for RHIC as stand-alone technique or to complement electron cooling [6], acting mainly on halo particles for which electron cooling approach is less efficient. OSC and its transit-time method were suggested to extend the stochastic cooling technique into the optical domain, with broad-band optical amplifier and undulator (wigglers) for coupling the optical radiation to charged-particle beam. Cooling results from a particle's interaction in the kicker undulator with its own amplifier radiation, emitted in the pickup undulator. The path of the particles between the pickup and kicker (called a bypass) can be designed such that each particle receives a correction kick from its own amplifier radiation toward equilibrium orbit and energy. The interaction of a particle with amplified radiation from other particles results in heating. It was shown in [7] that the balance between cooling and heating define the optimal power of amplifier needed to achieved the ultimate cooling rate that is limited only by the bandwidth of the cooling loop, pickup-amplifier-kicker. However, in all possible applications of OSC to heavy particles, including ^{79}Au ions in the RHIC, the power required in such system appears to be several orders of magnitude large then that feasible with modern optical amplifier. In this case, the amplifier's power limits the cooling time.

We define $X=(x,x',s,\delta)^T$ as the particle 4D coordinate vector, where x,x' are transverse coordinates and angles, s is the longitudinal coordinate, δ is the particle's relative energy offset. We identify the pickup undulator at a position A in the optics of the storage ring, and the kicker undulator at the position B . The beam transport from A to B can be written as $X_B=RX_A$. Consequently, $X_A=R^{-1}X_B$ and we define

$$R^{-1} = \begin{bmatrix} R_{11} & R_{12} & 0 & R_{16} \\ R_{21} & R_{22} & 0 & R_{26} \\ R_{51} & R_{23} & 1 & R_{56} \\ 0 & 0 & 0 & 1 \end{bmatrix} \quad (3.2.1)$$

The path-length difference on the trajectory from A to B written in terms of particle coordinates at a location B and taken relative to the equilibrium orbit is equal to

$$\Delta\ell = -(R_{51}x + R_{52}x' + R_{56}\delta) \quad (3.2.2)$$

This signal must be delayed to let the particle enter the kicker undulator ahead of the signal. Moreover, the path length for a signal including the delay in the amplifier must be chosen such that the equilibrium particle comes to the kicker undulator exactly at the crossover of the electric field with the electromagnetic wave of the signal. Then, the phase difference for a nonequilibrium particle is equal to

$$\varphi = \Delta\ell \frac{2\pi}{\lambda}, \quad (3.2.3)$$

where λ is wavelength of the undulator radiation. The particle energy right after the energy kick is

$$\delta = \delta + G \sin(\varphi), \quad (3.2.4)$$

where $G = -\Delta E / E_b$ is the gain amplifier, E_b is the beam energy. For simple calculation G is defined as

$$G = G_0 \cdot \Delta t \cdot \exp\left(-\frac{s - z_0}{2\sigma_z}\right), \quad (3.2.5)$$

Δt is time step of calculation, G_0 is input parameter in the unit δ/sec , z_0 and σ_z are parameters of the ion bunch.

The visual form for input the OSC parameters is presented in the Fig. 3.4.

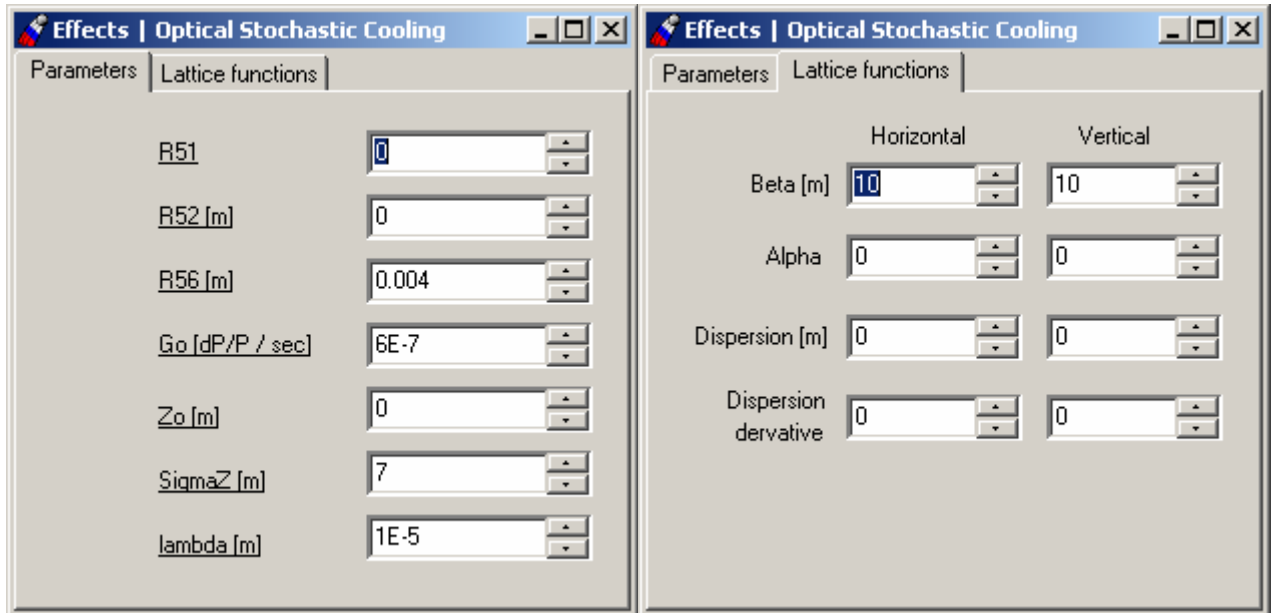


Fig.3.4. Input parameters for Optical Stochastic Cooling object.

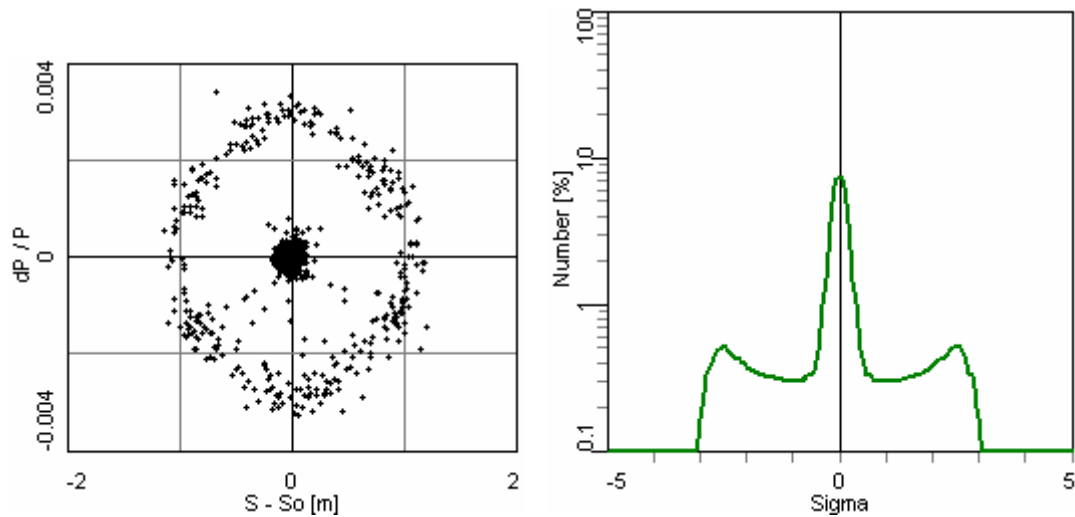


Fig. 3.5. Example of simulation using of Optical Stochastic Cooling: particle distribution in the longitudinal phase space (left) and longitudinal profile (right).

References

1. I.N.Meshkov, A.O.Sidorin, A.V.Smirnov, E.M.Syresin, G.V.Trubnikov, P.R.Zenkevich," SIMULATION OF ELECTRON COOLING PROCESS IN STORAGE RINGS USING BETACOOOL PROGRAM" , proceedings of Beam Cooling and Related Topics, Bad Honnef, Germany, 2001.
2. I.N.Meshkov, R. Maier et al, "Electron cooling application for luminosity preservation in an experiment with internal targets at COSY", Dubna 2001, Jul-4031.
3. B.Autin, "Fast betatron cooling in antiproton accumulator", CERN/PS-AA/82-20
4. H.Stockhorst, Design deliberations for a stochastic cooling system at HESR, FZJ
5. T.Katayama and N.Tokuda, Part. Acc., 1987, Vol. 21
- 6.M.Babzien, I.Ben-zvi, I.Pavlishin, I.Pogorelsky, V.Yakimenko, A.Zholents, M.Zolotorev. Optical stochastic cooling for RHIC using optical parametric amplification. Phys.Rev. volume 7, PRST-AB (2004).
7. D.Möhl, CERN Accelerator School Report, CERN 87-03 (1987), p.453.